

A new adaptive bending method using closed loop feedback control

T. WELO, B. GRANLY

Department of Engineering Design and Materials, Norwegian University of Science and Technology (NTNU),
Richard Birkelands veg 2B, N-7491 Trondheim, Norway

Received 23 October 2009; accepted 30 March 2010

Abstract: As the competition from companies in low cost countries increases, the need for more automated production which reduces labour cost while improving product quality is required. A new rotary compression bending set-up with automated closed-loop feedback control is thus being developed. By transferring in-process measurement data into an algorithm for predicting springback and bend angle prior to the unloading sequence, the dimensional accuracy is improved. This work focuses on the development of this steering model. Since the method used does not increase cycle time, it is attractive for high-volume industrial applications. More than 150 bending tests of AA6060 extrusions were conducted to determine the capability of the technology. The results show that by activating the automated closed-loop feedback system, the dimensional accuracy of the bent parts is more than three times better than that obtained by traditional compression bending. Since the steering model permits the direct use of additional process data, such as instant wall thickness and cross sectional distortions, it is believed that extension of the measurement capabilities would improve the accuracy of the methodology even further.

Key words: adaptive bending; closed-loop feedback; dimensional accuracy; springback; aluminium; extrusion

1 Introduction

1.1 Motivation and objective

As a result of the intensified globalisation in the market and supply bases, manufacturing companies are currently challenged with increased cost pressure. For companies in high cost countries, one way of facing this challenge is to apply more advanced and automated technologies which increase product quality while reduce labour cost. In the automotive industry, for example, improved shaping capabilities may increase functionality and product performance, including strength, stiffness, durability and crashworthiness while reducing system cost due to part consolidation and reduction of assembly operations such as welding. By converting from using traditional steel to using aluminium, the conflicting demand of adding more safety and luxury features, while lowering gas consumption (due to environmental concerns and legislations) can be achieved. However, due to the high material price compared with steel, product design should be optimized to minimize material consumption and provide more value to customers in terms of low weight and cost. The manufacturing and

quality cost of a new product may be reduced by using advanced manufacturing technology for improved dimensional accuracy. In this field, controlling springback represents a great challenge, with particularly two issues of interest[1]: dimensional targeting, where the goal is to produce a dimensionally correct part under standard conditions, and dimensional accuracy which deals with the variability (noise) in the process. The method developed herein is targeting at gaining improvement in both areas.

During bending of profiles, in-process measurements of torque and rotation are transferred into a steering model, which like Ref.[2], uses these indirect measurements of springback to calculate the required bending angle for achieving correct geometry after unloading. Unlike conventional compression bending, where the final angle before unloading is determined based on experience from previous bending trials, this method allows the operation to adapt to the specific material properties of the profile being bent. Since all measurements are done in-process, the cycle time is not affected, making it applicable for high volume production. The objective of this study is to present the development of the steering model for adaptive

compression bending of aluminium alloy profiles.

1.2 Overview of set-up

The lay-out of the rotary compression bender used in this study is shown in Fig.1[3]. It includes an electric power unit that is connected to a gear box. A torque transducer is placed between the exit of the gear box and the entry shaft of the upper bending arm. The rotation of the bending arm is measured using a rotational transducer connected to the gear. A drawback arrangement is mounted at the underside of the bending arm to eliminate the effect of friction. The lower tool is fixed and has a constant radius. A ridge is integrated in the contact surface of the tool to make an imprint along the inner flange of the profile.

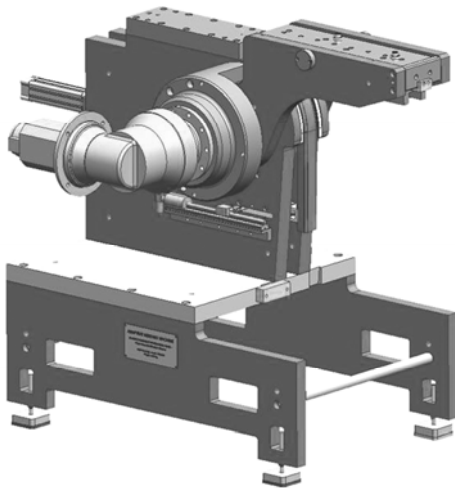


Fig.1 Outline of bending machine and tooling

2 Developing steering model

The first step in developing a steering model for

adaptive bending is to establish an analytical relationship between the applied moment (M) and the curvature (κ) of the section. This model will be used in the continuation to determine the distribution of the forces along the bent profile upon forming, combining appropriate boundary conditions and compatibility equations. Once the force distribution is known, springback deformations can be calculated by considering the change of forces between the loaded and the unloaded state of the profile, using elastic calculations with forces from the plastic loading process as input. The main steps required for establishing a closed loop steering model for springback compensation is shown in Fig.2.

2.1 Developing analytical moment–curvature model

During the inelastic forming of a part, it is assumed that the total strain can be represented by an elastic and a plastic component, where the plastic component is considerably larger than the elastic one during forming. In order to develop a model for prediction of moment versus curvature, a model that relates strain components to stress is required. Assuming that initially plane sections remain plane during plastic deformation, the following model applies

$$\varepsilon = \kappa y \tag{1}$$

where κ is the global curvature of the profile and y is the radial distance from the identified position of the neutral layer to any point considered in the plane of the cross section of the profile. In the first place, consider plastic bending of a massive rectangular cross section with depth (H) and width (B), assuming a state of one dimensional stress and that the material obeys LUDWIK’s simple constitutive law[4]. Equilibrium in the plane of the cross section means that the following relationship holds

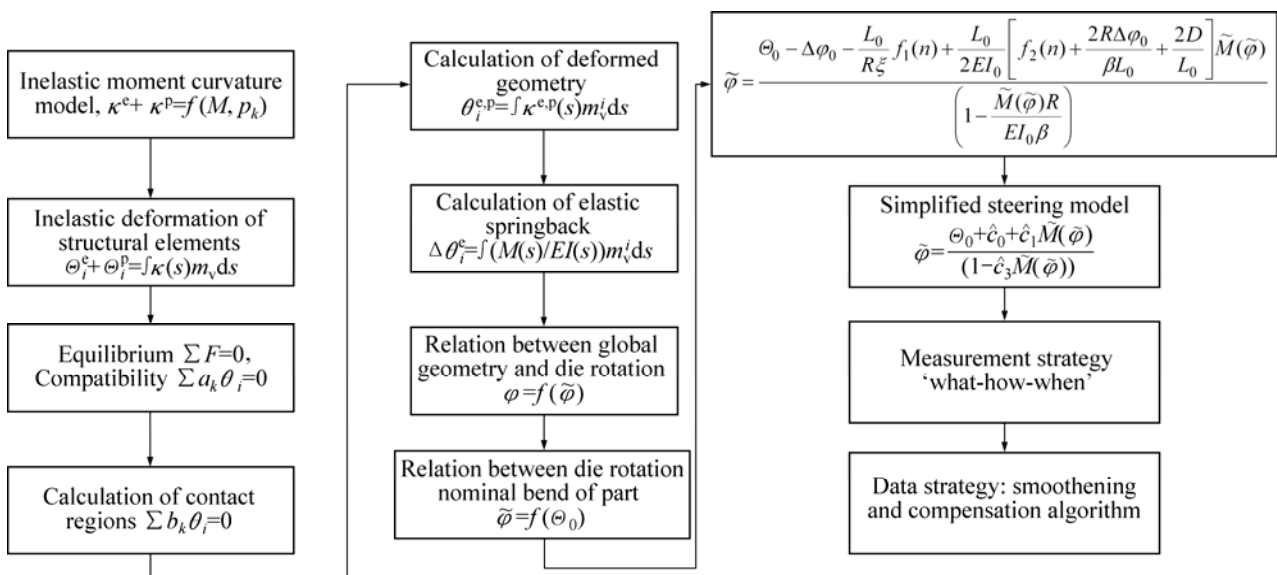


Fig.2 Steps for establishing closed loop steering model for springback compensation in compression bending

$$M^* = \int_{-H/2}^{H/2} \sigma y dA = \int_{-H/2}^{H/2} \sigma(\varepsilon) y B dy = \int_{-H/2}^{H/2} K(\kappa y)^n y B dy \tag{2}$$

In this relation, n is strain hardening coefficient and K is strength coefficient in LUDWIK's law. In case of a symmetric, rectangular hollow section, the geometry can be represented by the depth dimension of the internal chamber h and the corresponding width of the internal chamber b , in addition to the outside dimensions B and H . The applied bending moment, M , is found through the relation $M=M^*-m^*$. M^* and m^* are then the moments which would have been the case if the section was massive with height $H/2$ and $h/2$, respectively. When primarily searching for a relationship that can be used to resolve the force distribution by using compatibility equations, our objective is to search for a relationship in the form $\kappa=f(M)$, which can easily be integrated to determine deformations. This is achieved by simplifying the equation of the resulting moment using the first order terms of the Taylor series before solving the relationship with respect to plastic curvature. The resulting plastic curvature is thus

$$\kappa_p = \frac{2}{h} \psi \left(\frac{M}{M_k} \right)^{1/n} \tag{3}$$

$$M_k = KZ_c$$

$$\psi = \left[\frac{(n+2)}{2 \left(1 + n \frac{t}{h} \frac{Z^2 + z^2}{Z_c^2} \right)} \right]^{1/n}$$

Notice that the first area moment of the cross section is denoted $Z=BH^2/4$, and the term $Z_c=Z-z$ represents the first area static moment of the net rectangular hollow section.

In order to find the contribution to the compatibility equations, from the elastic deformations, the relationship for elastic curvature is searched for, using theory of elastic bending:

$$M = \int_A \sigma y dA = \int_A E \varepsilon_e y dA = \int_A E \kappa_e y^2 dA = E \kappa_e \int_A y^2 dA = EI \kappa_e \rightarrow \kappa_e = \frac{M}{EI} \tag{4}$$

where E is elastic modulus defining the stiffness of the material in the elastic region, I is second moment of area of the section and κ_e is elastic curvature representing the recoverable portion of the curvature upon release of bending moments during unloading. It may now be assumed that the total curvature is the summation of the elastic and plastic curvature components ($\kappa=\kappa_e+\kappa_p$). By

introducing Eqs.(3) and (4), this yields an approximate closed-form relationship that can be used to evaluate deflections during forming:

$$\kappa = \frac{M}{EI} + \frac{2}{h} \psi \left(\frac{M}{M_k} \right)^{1/n} \tag{5}$$

2.2 Defining structural and kinematically admissible deformation model for outer profile segment

The layout of the structural and kinematic model prior to unloading, including key dimensions, is shown in Fig.3. When forming the profile by imposing a rotation to the upper die, the bending moment along the end segment increases gradually from the main contact point between the profile and the upper die towards the contact point with the circular lower die. Due to these bending actions, the profile will deform according to the moment curvature characteristic, providing elastic and plastic deformation that will contribute to the overall shape after forming. Moreover, as a result of the deformations during bending, the theoretical contact point, as determined by the bend angle imposed, will be different from the real contact point. This means that the bend angle of the profile will be different from the imposed bend angle.

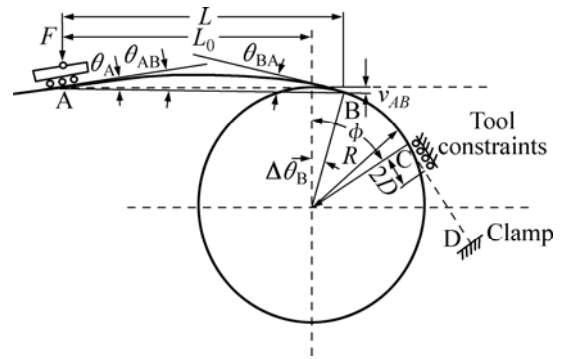


Fig.3 Layout of structural and kinematical model prior to unloading, including key dimensions (v_{AB} —Offset of point B relative to A; L —Length of segment; $\Delta\theta_B$ —Angle made up of tangent of bending die at contact point and global horizontal line; L_0 —Distance from A to theoretical contact point in case profile had remained straight; R —Characteristic die radius)

The main task is thus to determine the angle $\Delta\theta_B$ which represents a certain portion of the bend angle needed for the profile to deform into the radius of the die; i.e. defining the contact point between the profile and the die at the outer end of the bend. The first step to resolve this challenge is to establish compatibility equations for this segment. Using a curvature momentum approach, it may be shown that the angle θ_{BA} made up by the rotation at end B of segment BA relative to a chord taken between those two end points is

$$\theta_{BA} = \int_L \kappa(s)M_v(s)ds \tag{6}$$

where $\kappa(s)$ is the curvature as a function of the coordinate s , and $M_v(s)$ is a virtual, or weight function. Because $\Delta\theta_B$ and v_{AB} are small quantities compared with the imposed bend angle, approximations can be made. According to Fig.3, compatibility at B then requires that

$$\theta_{BA} = \Delta\theta_B - \frac{v_{AB}}{L} = \frac{L-L_0}{R} - \frac{(L-L_0)^2}{2RL} \tag{7}$$

Assuming that the profile takes the characteristic radius of the bending die inside the contact point B, the second compatibility equation is then obtained:

$$\kappa(M_B) = \frac{1}{R} \approx \frac{\partial^2 v}{\partial s^2} \Big|_B \tag{8}$$

It should be noted that a condition for the profile to contact the lower die in the center segment of the bend is that the contact stress and force distribution provide a constant bending moment over the segment, and that the effect of friction can be neglected. The next step is to determine $\Delta\theta_B$ by first realizing that:

$$\theta_{BA} = \int_L \kappa(s)M_v(s)ds \approx \int_L \kappa(x)M_v(x)dx \tag{9}$$

or, by inserting relation for the moment and weight function:

$$\theta_{BA} = \int_L \left[\frac{M_B}{EI} \left(\frac{x}{L} \right) + \psi \frac{2}{h} \left(\frac{M_B}{M_k} \frac{x}{L} \right)^{1/n} \right] \left(\frac{x}{L} \right) dx \tag{10}$$

where the moment curvature model developed in Section 2.1. has been adopted, M_B is the applied moment at point B and the weight function is x/L . Evaluating the above integral, combining this equation with the rewritten version of the first compatibility equation and introducing the dimensionless quantity $\zeta=L_0/L$, the above equation reads

$$\theta_{BA} = \frac{L}{3} \left[\frac{1}{R} - \psi \frac{2}{h} \left(\frac{-1+1/n}{2+1/n} \right) \left(\frac{M_B}{M_k} \right)^{1/n} \right] = \frac{1-\zeta}{R} - \frac{(1-\zeta)^2}{2R} \tag{11}$$

Notice that the second term inside the square bracket is proportional to the plastic curvature at B. When considering this in relation to the total curvature locally at B, this means that the plastic curvature is much larger than the elastic curvature, meaning that the latter can be neglected for this single purpose only. The expression gained can then be solved with respect to ζ , resulting in the simple solution:

$$\zeta = \sqrt{\frac{1/n}{2+1/n}} = \sqrt{\frac{1}{2n+1}} \tag{12}$$

Using the approximation of $\Delta\theta_B$ from Eq.(7), the above result may be rewritten into the following form

$$\Delta\theta_B = \frac{L_0}{R} \frac{1-\zeta}{\zeta} \tag{13}$$

where all parameters are uniquely determined. The interpretation of this final result is that it will take a longer distance (or angle) for the profile to deform into the die radius if the bending arm is made longer. It may also happen, depending on the material characteristic and the imposed bend angle, that $\Delta\theta_B$ gets larger than the imposed bend angle, meaning that the profile will never be able to take the radius of the die. Hence, the solution obtained above is only valid if $\Delta\theta_B < \theta_0$ where the imposed angle is denoted θ_0 .

2.3 Defining structural and kinematic admissible deformation model for clamped profile segment

When the profile is loaded in the adaptive bending machine, the extreme end is clamped to prevent it from rotating as well as move axially when the bending load is applied. At end C of the considered profile segment where the circular forming die is located, the profile is not free to deform under the action of bending. The reason for this is that the circular forming die has a circumferential, protruding ridge going all the way along the bending die. Moreover, different from the outer end, an upper die channel prevents the profile from deforming outwards. When forming starts, the protruding ridge immediately gets into contact with the lower flange of the profile. Due to the combined effect from concentrated contact stresses, compressive bending stresses and a relatively thin-walled cross section, a dimple is immediately formed along the lower flange upon bending. Hence, the considered profile segment is clamped between the lower die and the outer channel wall of the tool, resembling the situation of placing a bar in a vice and bending it by applying a transverse force.

The main challenge associated with establishing a structurally and kinematically admissible model is evaluating the force distribution within the clamped region as well as the extension of the clamped region. As a start let us accept the model established for the outer segment of the profile (A-B). In doing so, the requirement for the profile to be in perfect contact with the circular die over the angle $\theta_0 - \Delta\theta_B$, is the condition for constant bending in this region. This means that the combined effect of the bending force applied from the rotating and the contact pressure ($q(\theta)$) must produce a constant bending moment along the bend. As a consequence, the transverse shear force at any point

along the constantly bent segment must be zero, leading to the conclusion that the shear force at the clamped end of the profile (C) must be zero.

Fig.4 illustrates a structurally admissible distribution of forces in the clamped region of the formed profile. However, the contact stress, its distribution and extension with the clamped region are all unknown, and more importantly, there are no known methods to solve the contact problem exactly. Notwithstanding the conditions of the clamped profile resemble the extreme imagined situation where the bar is flexible more than the other extreme where the material of the bar is stiffer than the material of the shims. In this case, the corresponding contact stresses between the shims and the bar would produce more rectangular stress blocks as the extreme case.

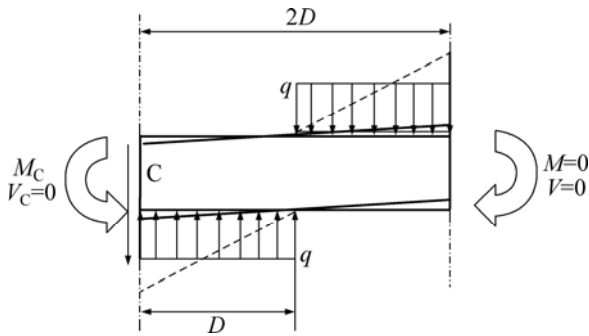


Fig.4 Structurally admissible distribution of forces in clamped region of formed profile

In the continuation, the assumption of rectangular contact stress blocks will be used to establish a structural model. Let us first assume that the bending moment is known ($M_B=M_C$), and that the transverse shear force V_C is zero. A criterion for the bending moment to be ‘absorbed’ within the clamed area of assumed length $2D$ can be established directly from equilibrium considerations:

$$-M_C + qD \frac{3D}{2} - qD \frac{D}{2} = 0 \tag{14}$$

When assuming that the profile has to take the shape made up of the upper and lower dies, it may be argued that the ‘global shape’ of the profile must remain straight during bending. This may be a correct assumption, but in this connection one should also consider the fact that the forces generated during bending will be released when removing the forming load and releasing the part from the tools. This means that the bending moment distribution gives rise to stresses that will be released upon unloading, which in turn affect the overall springback of the part. Since the clamped region is located close to the centre of the bend, establishing a correct model for the force distribution within the

clamped region is essential to the accuracy of an adaptive steering model.

2.4 Defining model for calculation of springback of overall system

We start by establishing a method for prediction of the change of bend angle when releasing the forces from the profile during unloading, assuming that the starting geometry is known. Using the moment curvature method along with the results established in Sections 2.1–2.3, the change of slope as represented by the total elastic curvature area taken between the end points A and D of the profile can be predicted from the following relationship, using the previously introduced notation:

$$\Delta\theta_{A-D}^s \equiv \Delta\theta_{AD}^s + \Delta\theta_{DA}^s = \int_{\text{system}} \kappa_e(s) ds \tag{15}$$

Here, κ_e is the elastic curvature from bending of the profile, and s is a longitudinal coordinate assumed to follow the deformed profile. By assuming that $s \approx x$ along the almost straight segment of the profile, $R\theta \approx s$ along the circular segment of the deformed profile, and splitting the system into three separate regions, the following relationship holds

$$\Delta\theta_{A-D}^s = \int_0^L \frac{M_B}{EI_0} \left(\frac{x}{L} \right) dx + \int_0^{\theta_0 - \Delta\theta_B} \frac{M_B}{EI} R d\theta + \int_0^{2D} \frac{M_C}{EI_0} \left(1 - \frac{x'}{2D} \right) dx' \tag{16}$$

where EI_0 is the initial stiffness of the section, whereas EI is the stiffness of the crushed cross section in the central bend region. Notice that the origin of coordinated x is at A, whereas the origin of coordinate x' is at C. Using the relationship between L and L_0 , in addition to defining a new parameter $I = \beta I_0$ where $\beta < 1$, the equation is simplified before a straightforward integration is conducted. Adding previous calculation of $\Delta\theta_B$ may be used to further rearrange and simplify the solution into the following explicit, closed-form relationship representing overall change of slope during unloading:

$$\Delta\theta_{A-D}^s = \frac{1}{2} \frac{M_B}{EI_0} \left[\left(\frac{L_0}{\xi} \right) \left(1 - \frac{1-\xi}{\beta} \right) + \frac{2R\theta_0}{\beta} + 2D \right] \tag{17}$$

Since the steering model is going to operate in real time, it is necessary to determine a relationship for prediction of the part geometry prior to unloading, and then relate this to the imposed (predetermined) bend angle, as well as the geometry of the final part. Adopting the moment curvature model developed in Section 2.1, as well as the curvature area method for finding slopes and deflections shown in Section 2.2, it may be shown that the searched angle may be found by evaluating the following integral:

$$\theta_{AB} = \int_L \left[\frac{M_B}{EI} \left(\frac{x}{L} \right) + \psi \frac{2}{h} \left(\frac{M_B x}{M_k L} \right)^{1/n} \right] \left(1 - \frac{x}{L} \right) dx \quad (18)$$

where M_B is the applied moment at point B and the weight function is $(1-x/L)$ since we are searching the rotation in end A. Evaluate the above integral and determinate the true deflection slope at end A relative to the rotation of the former die (see Fig.3). Making use of the expression developed for θ_{AB} and that the total curvature can be simplified into $1/R$, the relationship can be simplified into

$$\theta_A = \frac{M_B L}{6EI} + \frac{L_0}{R\xi} \left[\left(\frac{n^2}{(n+1)(2n+1)} \right) - \frac{1}{2} (1-\xi)^2 \right] \quad (19)$$

The next step is then to relate the true relative angle at A relative to the rotation of former die (θ_A) to the final bend angle after unloading, θ_{A-D}^r . In this case, we then get the following geometrical relationship:

$$\theta_{A-D}^r = \overbrace{\theta_0^{\text{die rotation}} + \frac{L_0}{R\xi} \left[\left(\frac{n^2}{(n+1)(2n+1)} \right) - \frac{1}{2} (1-\xi)^2 \right]}^{\text{difference between profile and die rotations}} - \overbrace{\left[\frac{1}{2} \frac{M_B L_0}{EI_0} \left[\left(\frac{1}{\xi} \right) \left(\frac{2}{3} - \frac{1-\xi}{\beta} \right) + \frac{2R\theta_0}{\beta L_0} + 2 \frac{D}{L_0} \right]}^{\text{conventional springback terms}} \right]} \quad (20)$$

In order to find the desired rotation of the die prior to unloading, Eq.(20) is solved with regard to the die rotation at end of forming ($\tilde{\varphi}$). Before the bending operation begins, the die will rotate from the starting position until it reaches contact with the profile surface. The geometrical relation is thus $\theta_0 = \tilde{\varphi} + \Delta\varphi_0$, where $\Delta\varphi_0$ is the difference between the initial rotation of the die and the profile. Assuming that the theoretical torque equals the measured torque in point B during bending, we have $M_B = \tilde{M}(\tilde{\varphi})$. Using the relations between the theoretical and measured variables, the resulting steering model is as follows:

$$\tilde{\varphi} = \left\{ \theta_0 - \Delta\varphi_0 - \frac{L_0}{R\xi} \left[\left(\frac{n^2}{(n+1)(2n+1)} \right) - \frac{(1-\xi)^2}{2} \right] + \frac{L_0}{2EI_0} \left[\left(\frac{1}{\xi} \right) \left(\frac{2}{3} - \frac{1-\xi}{\beta} \right) + \frac{2R\Delta\varphi_0}{\beta L_0} + \frac{2D}{L_0} \right] \tilde{M}(\tilde{\varphi}) \right\} / \left(1 - \frac{\tilde{M}(\tilde{\varphi})R}{EI_0\beta} \right) \quad (21)$$

where θ_0 is the targeted angle and n is the strain hardening parameter. In case the measurements include die rotation and torque only, all variables that are

independent of these are collected into constants, and the above equation may be simplified into

$$\tilde{\varphi} = \frac{\Theta_0 + \hat{c}_0 + \hat{c}_1 \tilde{M}(\tilde{\varphi})}{1 - \hat{c}_3 \tilde{M}(\tilde{\varphi})} \quad (22)$$

When constructing the adaptive bending machine and applying the steering model, one has to take account of the accuracy, stability and roughness of the measuring devices. A strategy for registering, smothering, converting, and feeding data into the steering model also need to be established. However, this is a long discussion that goes beyond this work.

2.5 Calibration and test procedures

Since the torque ($M(\varphi)$) and rotation (φ) are measured directly on the shaft that connects the gear and the bending arm, the effects of gravity forces ($M_g(\varphi)$) and bearing friction ($M_\mu(\varphi, \Delta_i)$) have to be eliminated, hence

$$M(\varphi) - M_p(\varphi) = \pm M_\mu(\varphi, \Delta_i) - M_g(\varphi) \quad (23)$$

where $M_p(\varphi)$ is the bending resistance of the profile. After calibrating the moment readings, additional machine cycles were run without profile to determine robustness. After forming, a digital protractor was used to measure the final bend angle. The repeatability of the procedure was checked by performing a number of consecutive measurements on the same profile. The bent shapes were measured in a simple fixture. Thin-walled, rectangular hollow AA 6060-T1 profiles were used in the tests. In order to provoke different material characteristics, the profiles were aged to different temper conditions, including ‘as is’ (T1 condition), and, respectively, 60 min and 120 min at 175 °C, providing a $\pm 17\%$ range in yield stress. The test overview is listed in Table 1.

Table 1 Test overview

Series No.	Control model	Heat treatment	Number of profiles
1	Manual	“As is”	25
2	Manual	175 °C, 60 min	25
3	Manual	175 °C, 120 min	25
4	Adaptive	“As is”	25
5	Adaptive	175 °C, 60 min	19
6	Adaptive	175 °C, 120 min	20

3 Validation of dimensional capabilities

A summary of the results obtained from more than 140 tests is given in Table 2. For the adaptive process, the targeted angle (θ_0) was 80°, whereas the traditional

process was run with a pre-specified bend angle (φ) of 85° without any attempts made to hit the same nominal. Assuming a tolerance band of 1.0° , the adaptive process shows a dimensional process capability that is more than three times better than the traditional process. If the bend angle is a standard dimensional feature (with $C_p > 1.33$) of a specific part, the traditional process would require a tolerance band of 3.26° , whereas the adaptive process would only need a tolerance of $\pm 0.53^\circ$ in order to provide good parts. This result clearly demonstrates that adaptive processing has a high industrial potential for improving part quality and reducing quality cost.

Table 2 Result summary

Parameter	Traditional process	Adaptive process
Average angle, $\theta/(^\circ)$	80.75	79.82
Max angle, $\theta_{\max}/(^\circ)$	81.32	80.05
Min angle, $\theta_{\min}/(^\circ)$	80.05	79.60
Standard deviation of $\theta/(^\circ)$	0.41	0.13
$C_p(\pm 0.5^\circ)/(^\circ)$	0.41	1.25
USL–LSL ($C_p=1.33$)/(°)	3.26	1.06

4 Conclusions

1) An adaptive forming technology with closed-loop feedback control has been developed. The technology is aimed at high volume applications.

2) The technology provides dimensional tolerance capability that is approximately 3 times better than that of conventional processes.

3) Since the steering model permits the use of additional process data, such as instant wall thickness and cross sectional distortions, it is believed that extension of the measurement capabilities would improve the accuracy of the methodology even further. Improvement potentials have thus been identified as: increase number of measuring parameters, improve measurement strategy and refinement and further work on steering model.

References

- [1] WELO T. Bending of aluminum extrusions for automotive applications: A commentary on theoretical and practical aspects [J]. Proc 6th Int Aluminium Extrusion Technology Seminar. Chicago, USA, 1996: 271.
- [2] ZHU H, STELSON K A. Modeling and closed-loop control of stretch bending of aluminum rectangular tubes [J]. Journal of Manufacturing Science and Engineering, 2003, 125: 113–119.
- [3] WELO T, SÆTERTRØ K, SØVIK O P. Adaptive bending of aluminum extrusions using an automated closed-loop feedback approach [C]//11th Int Esaform Conference on Material Forming. Lyon, France, 2008.
- [4] LUDWIK P. Technologische studie über blechbiegung [J]. Technische Blatter, 1903: 133-159.

(Edited by YANG Bing)